PTEP

Prog. Theor. Exp. Phys. **2022** 093B08(13 pages)
DOI: 10.1093/ptep/ptac113

IYBSSD2022
International Year
of Basic Sciences
for Sustainable Development

Study of *F*-wave bottom mesons in heavy quark effective theory

Ritu Garg* and A. Upadhyay

School of Physics and Materials Science, Thapar Institute of Engineering and Technology, Patiala - 147004, Punjab, INDIA

*E-mail: rgarg_phd19@thapar.edu

Received July 11, 2022; Accepted August 25, 2022; Published August 27, 2022

We study *F*-wave bottom mesons in heavy quark effective theory. The available experimental and theoretical data is used to calculate the masses of *F*-wave bottom mesons. The decay widths of bottom mesons are analyzed to find upper bounds for the associated couplings. We also construct Regge trajectories for our predicted data in the (J, M^2) plane, and our results nicely fit on Regge lines. Our results may provide crucial information for future experimental studies.

Subject Index B60

1. Introduction

In the last 15 years, heavy-light hadrons have been explored experimentally as well as theoretically. In the D-meson family, several new states have been observed at different experimental facilities like LHCb, BaBar, BESIII, etc. which have enriched the charm spectrum. In 2021, LHCb observed the state $D^0_{s0}(2590)$ with mass $M = 2591\pm13$ MeV and decay width $\Gamma = 89\pm28$ MeV respectively [1]. They also assigned the state $D^0_{s0}(2590)$ with quantum number $n = 3$ and $l = 0$. Earlier, in 2010, many candidates like $D(2550)^0$, $D^*(2600)^{0,+}$, $D(2750)^0$, *and* $D^*(2760)^0$ were observed by the BaBar collaborations [2] and reconfirmed by LHCb in 2013 [3]. Furthermore, the LHCb collaborations in 2019 analyzed the four-body amplitude of decay $B^- \longrightarrow D^{*+}\pi^-\pi^+$ [4]. They reported the existence of charm resonances $D_0(2550)^0$, $D^*_1(2600)^0$, $D_2(2740)^0$, and $D^*_3(2760)$ with $J^P = 0^-, 1^-, 2^-$, and 3^-, respectively. In addition, LHCb(2013) also confirmed the states $D_J(3000)^0$ and $D^*_J(3000)^0$ with unnatural and natural parity, respectively [3]. In 2015, the LHCb collaborations discovered the state $D^*_1(2760)^0$ with $J^P = 1^-$ by studying $B^- \longrightarrow D^+\pi^-K^-$ decay [5]. However, the bottom meson family is still less abundant in experimental confirmations. The only ground state $B^{0,\pm}(5279)$, $B^*(5324)$, $B_s(5366)$, $B^*_s(5415)$, and a few orbitally excited states $B_1(5721)$ and $B^*_2(5747)$ are listed by the Particle Data Group [6]. In 2013, the CDF collaborations observed two higher resonances $B_J(5970)^{0,+}$ by analyzing the invariant mass distribution of $B^0\pi^+$ and $B^-\pi^+$ [7]. In 2015, LHCb observed the four resonances $B_1(5721)^{0,+}$, $B^*_2(5747)$, $B_J(5840)^{0,+}$, $B_J(5960)^{0,+}$ by analyzing the mass spectra $B^+\pi^-$, $B^+\pi^-$ in p–p collisions [8]. The properties of the state $B_J(5960)^{0,+}$ [8] are consistent

Funded by SCOAP[3]. SCOAP3 and OUP support the goals of the International Year of Basic Sciences for Sustainable Development

with the state $B_J(5970)^{0,+}$ of CDF(2013) [7]. In the B_s family, the ground state and 1P(1^+, 2^+) are well established. Recently, LHCb detected the D-wave state B_s^0 with two peaks of mass 6061±1.2±0.8 MeV and 6114±3±5 MeV in the B^+K^- mass spectrum [9]. Apart from this, there is no experimental information for higher excited states until now.

In theory, various theoretical studies like masses, strong decays, radiative decays, weak decays, and spin-parity value (J^P) have been performed for higher excited bottom mesons with different models [10–38]. In the B-meson family, the states $B^0(5279)$, $B^{\pm}(5279)$, $B^*(5324)$, $B_s(5366)$, $B_s^*(5416)$ are well established and classified as $1S$ states. In addition, the states $B_1(5721)$, $B_2^*(5747)$ are experimentally confirmed and identified as $1P(1^+, 2^+)$ respectively. But there are puzzles for placing the newly observed states $B_J(5840)^{0,+}$, $B_J(5960)^{0,+}$ in spectra. In the literature, different theoretical models give different assignments for these states based on predicted masses and decay widths reported by the CDF and LHCb experimental groups. The newly observed state $B_J(5840)$ was analyzed with a quark model and favored the assignment of $B(2^1S_0)$ [24,25]. But $^3P_0$ decay model analysis suggested the assignment of state $B_J(5840)$ as $B(2^3S_1)$ [28], while heavy quark effective theory (HQET) has explained the resonances $B_J(5840)$ as the $B(1^3D_1)$ state [37]. The state $B_J(5960)^{0,+}$ can be assigned to $B(2^3S_1)$ with the relativistic quark model [11,22], while some other models suggested it to be the second orbitally excited 1^3D_3 [24,28] state or 1^3D_1 state [25]. There is also ambiguity for recently observed strange bottom meson states $B_{sJ}(6064)$ and $B_{sJ}(6114)$. Bing Chen et al. [39] studied the states $B_{sJ}(6064)$ and $B_{sJ}(6114)$ with a non-relativistic quark potential model and suggested them to be D-wave states. Theoretical studies for these states are limited for now, which indicates they need more attention. The experimental progress has stimulated the interest of theorists to check the validity of the theoretically available models for these upcoming data. It also motivates us to explore the mass spectrum theoretically for missing states and fill the voids in the spectrum.

In this paper we study the properties of the $1F$ state by exploring HQET, an effective theory that describes the dynamics of heavy-light hadrons. In this theory, two kinds of approximate symmetries are incorporated: heavy quark symmetry (HQS) and chiral symmetry of light quarks. The detailed information for HQET is discussed in Sect. 2. Recent data has motivated us to study the $1F$ states' properties. In this paper we predict the masses and upper bounds of the associated couplings for the $1F$ state. We analyze the decay behavior of the $1F$ states with pseudoscalar mesons and calculate an upper bound on the associated couplings. In Sect. 2, HQET and its Lagrangian are briefly discussed. Using available data, masses and decay properties are studied in Sect. 3. In Sect. 4, the conclusions drawn from our study are provided.

2. Theoretical formulation

The study of heavy-light hadrons can be explored in the HQET framework. It is a powerful tool to describe the properties of heavy-light mesons like masses, decay widths, branching ratios, fractions, spin, parity, etc. The theory is explained with two approximate symmetries, heavy quark symmetry and chiral symmetry. Heavy quark symmetry is valid in the approximation $m_Q \to \infty$, where the spin of light quarks is decoupled from the spin of heavy quarks, so the total angular momentum of light quarks remains conserved. The total angular momentum of light quarks is $s_l = s_q + l$, with s_q = spin of light quark (1/2) and l = total orbital momentum of light quarks. In the heavy quark limit, mesons are grouped in doublets on the basis of the total angular momentum s_l of light quarks. For $l = 0$, $s_l = 1/2$ coupled this with the spin of the heavy quark $s_Q = 1/2$ and resulted in the doublet $(0^-, 1^-)$. This doublet is given by (P, P^*). For $l = 1$, two doublets are formed denoted by $(P_0^*, P_1^{'})$ and (P_1, P_2^*), with $J_{s_l}^P = (0^+, 1^+)$ and $J_{s_l}^P = (1^+, 2^+)$ respectively. For $l = 2$, two doublets are expressed by (P_1^*, P_2) and $(P_2^{'}, P_3^*)$ with $J_{s_l}^P = (1^-, 2^-)$ and $J_{s_l}^P = (2^-, 3^-)$ respectively. Similarly, for $l = 3$ we get the doublets (P_2^*, P_3) and $(P_3^{'}, P_4^*)$ for $J_{s_l}^P = (2^-, 3^-)$ and $J_{s_l}^P = (3^-, 4^-)$ respectively. These doublets are expressed in terms of super effective fields H_a, S_a, T_a, X_a^μ, $Y_a^{\mu\nu}$, $Z_a^{\mu\nu}$, $R_a^{\mu\nu\rho}$ [40]:

$$H_a = \frac{1+\not{v}}{2}\left\{P_{a\mu}^* \gamma^\mu - P_a \gamma_5\right\}, \tag{1}$$

$$S_a = \frac{1+\not{v}}{2}\left[P_{1a}^{'\mu}\gamma_\mu\gamma_5 - P_{0a}^*\right], \tag{2}$$

$$T_a^\mu = \frac{1+\not{v}}{2}\left\{P_{2a}^{*\mu\nu}\gamma_\nu - P_{1a\nu}\sqrt{\frac{3}{2}}\gamma_5\left[g^{\mu\nu} - \frac{\gamma^\nu(\gamma^\mu - \upsilon^\mu)}{3}\right]\right\}, \tag{3}$$

$$X_a^\mu = \frac{1+\not{v}}{2}\left\{P_{2a}^{\mu\nu}\gamma_5\gamma_\nu - P_{1a\nu}^*\sqrt{\frac{3}{2}}\left[g^{\mu\nu} - \frac{\gamma_\nu(\gamma^\mu + v^\mu)}{3}\right]\right\}, \tag{4}$$

$$Y_a^{\mu\nu} = \frac{1+\not{v}}{2}\left\{P_{3a}^{*\mu\nu\sigma}\gamma_\sigma - P_{2a}^{'\alpha\beta}\sqrt{\frac{5}{3}}\gamma_5\left[g_\alpha^\mu g_\beta^\nu - \frac{g_\beta^\nu\gamma_\alpha(\gamma^\mu - v^\mu)}{5} - \frac{g_\alpha^\mu\gamma_\beta(\gamma^\nu - v^\nu)}{5}\right]\right\}, \tag{5}$$

$$Z_a^{\mu\nu} = \frac{1+\not{v}}{2}\left\{P_{3a}^{\mu\nu\sigma}\gamma_5\gamma_\sigma - P_{2a}^{*\alpha\beta}\sqrt{\frac{5}{3}}\left[g_\alpha^\mu g_\beta^\nu - \frac{g_\beta^\nu\gamma_\alpha(\gamma^\mu + v^\mu)}{5} - \frac{g_\alpha^\mu\gamma_\beta(\gamma^\nu + v^\nu)}{5}\right]\right\}, \tag{6}$$

$$R_a^{\mu\nu\rho} = \frac{1+\not{v}}{2}\left\{P_{4a}^{*\mu\nu\rho\sigma}\gamma_5\gamma_\sigma - P_{3a}^{'\alpha\beta\tau}\sqrt{\frac{7}{4}}\left[g_\alpha^\mu g_\beta^\nu g_\tau^\rho - \frac{g_\beta^\nu g_\tau^\rho\gamma_\alpha(\gamma^\mu - v^\mu)}{7} - \frac{g_\alpha^\mu g_\tau^\rho\gamma_\beta(\gamma^\nu - v^\nu)}{7} - \frac{g_\alpha^\mu g_\beta^\nu\gamma_\tau(\gamma^\rho - v^\rho)}{7}\right]\right\}. \tag{7}$$

The field H_a shows the S-wave doublets for $J^P = (0^-, 1^-)$. The fields S_a and T_a describe the P-wave doublets for $J^P = (0^+, 1^+)$ and $(1^+, 2^+)$ respectively. D-wave doublets for $J^P = (1^-, 2^-)$ and $(2^-, 3^-)$ belong to the fields X_a^μ and $Y_a^{\mu\nu}$ respectively. In same manner, the fields $Z_a^{\mu\nu}$, $R_a^{\mu\nu\rho}$ present F-wave doublets for $J^P = (2^+, 3^+)$ and $(3^+, 4^+)$ respectively. In the above expresssions, a is the light quark (u, d, s) flavor index and v the heavy quark velocity, conserved in strong interactions. The approximate chiral symmetry $SU(3)_L \times SU(3)_R$ is involved with fields of the pseudoscalar mesons π, K, and η, which are the lightest strongly interacting bosons. They are treated as approximate Goldstone bosons of this chiral symmetry and can be introduced by the matrix field $U(x) = \exp\left[i\sqrt{2}\phi(x)/f\right]$, where $\phi(x)$ is given by

$$\phi(x) = \begin{pmatrix} \frac{1}{\sqrt{2}}\pi^0 + \frac{1}{\sqrt{6}}\eta & \pi^+ & K^+ \\ \pi^- & -\frac{1}{\sqrt{2}}\pi^0 + \frac{1}{\sqrt{6}}\eta & K^0 \\ K^- & \bar{K}^0 & -\sqrt{\frac{2}{3}}\eta \end{pmatrix}. \tag{8}$$

The fields of the heavy meson doublets given in Eqs. (1–7) interact with pseudoscalar Goldstone bosons via the covariant derivative $D_{\mu ab} = -\delta_{ab}\partial_\mu + \mathcal{V}_{\mu ab} = -\delta_{ab}\partial_\mu + \frac{1}{2}(\xi^+\partial_\mu\xi + \xi\partial_\mu\xi^+)_{ab}$ and axial vector field $A_{\mu ab} = \frac{i}{2}(\xi\partial_\mu\xi^\dagger - \xi^\dagger\partial_\mu\xi)_{ab}$. By including all meson doublet fields and

Goldstone fields, the effective Lagranigan is given by

$$\begin{aligned}\mathcal{L} = & \, i\text{Tr}\left[\overline{H}_b v^\mu D_{\mu ba} H_a\right] + \frac{f_\pi^2}{8}\text{Tr}\left[\partial^\mu U \partial_\mu U^+\right] \\ & + \text{Tr}\left[\overline{S_b}\left(iv^\mu D_{\mu ba} - \delta_{ba}\Delta_S\right) S_a\right] + \text{Tr}\left[\overline{T_b^\alpha}\left(iv^\mu D_{\mu ba} - \delta_{ba}\Delta_T\right) T_{a\alpha}\right] \\ & + \text{Tr}\left[\overline{X_b^\alpha}\left(iv^\mu D_{\mu ba} - \delta_{ba}\Delta_X\right) X_{a\alpha} + \text{Tr}\left[\overline{Y_b^{\alpha\beta}}\left(iv^\mu D_{\mu ba} - \delta_{ba}\Delta_Y\right) Y_{a\alpha\beta}\right] \\ & + \text{Tr}\left[\overline{R_b^{\alpha\beta\rho}}\left(iv^\mu D_{\mu ba} - \delta_{ba}\Delta_R\right) T_{a\alpha\beta\rho}\right]. \end{aligned} \tag{9}$$

The mass parameter Δ_F (where $F = S, T, X, Y, R$) in Eq. (9) represents the mass difference between higher-mass doublets (F) and the lowest-lying doublet (H) in terms of spin average masses of these doublets with the same principle quantum number (n). The expressions for the mass parameters are given by:

$$\Delta_F = \overline{M_F} - \overline{M_H}, \qquad F = S, T, X, Y, Z, R, \tag{10}$$

$$\text{where } \overline{M_H} = \left(3m^Q_{P_1^*} + m^Q_{P_0}\right)/4, \tag{11}$$

$$\overline{M_S} = \left(3m^Q_{P_1'} + m^Q_{P_0^*}\right)/4, \tag{12}$$

$$\overline{M_T} = \left(5m^Q_{P_2^*} + 3m^Q_{P_1}\right)/8, \tag{13}$$

$$\overline{M_X} = \left(5m^Q_{P_2} + 3m^Q_{P_1^*}\right)/8, \tag{14}$$

$$\overline{M_Y} = \left(5m^Q_{P_3^*} + 3m^Q_{P_2'}\right)/8, \tag{15}$$

$$\overline{M_Z} = \left(7m^Q_{P_3} + 5m^Q_{P_2^*}\right)/12, \tag{16}$$

$$\overline{M_R} = \left(9m^Q_{P_4^*} + 7m^Q_{P_3'}\right)/12. \tag{17}$$

The $1/m_Q$ corrections to the heavy quark limit are given by symmetry-breaking terms. The corrections are of the form

$$\begin{aligned}\mathcal{L}_{1/m_Q} = & \frac{1}{2m_Q}\Big[\lambda_H \text{Tr}\left(\overline{H}_a\sigma^{\mu\nu}H_a\sigma_{\mu\nu}\right) + \lambda_S \text{Tr}\left(\overline{S}_a\sigma^{\mu\nu}S_a\sigma_{\mu\nu}\right) + \lambda_T \text{Tr}\left(\overline{T}_a^\alpha\sigma^{\mu\nu}T_a^\alpha\sigma_{\mu\nu}\right) \\ & + \lambda_X \text{Tr}\left(\overline{X}_a^\alpha\sigma^{\mu\nu}X_a^\alpha\sigma_{\mu\nu}\right) + \lambda_Y \text{Tr}\left(\overline{Y}_a^{\alpha\beta}\sigma^{\mu\nu}Y_a^{\alpha\beta}\sigma_{\mu\nu}\right) \\ & + \lambda_Z \text{Tr}\left(\overline{Z}_a^{\alpha\beta}\sigma^{\mu\nu}Z_a^{\alpha\beta}\sigma_{\mu\nu}\right) + \lambda_R \text{Tr}\left(\overline{R}_a^{\alpha\beta\rho}\sigma^{\mu\nu}R_a^{\alpha\beta\rho}\sigma_{\mu\nu}\right)\Big]. \end{aligned} \tag{18}$$

Here, the parameters λ_H, λ_S, λ_T, λ_X, λ_Y, λ_Z, λ_R are analogous to hyperfine splittings and defined as in Eqs. (14–25). The mass terms in the Lagrangian represent only the first order in $1/m_Q$ terms, but higher-order terms may also be present. We are restricting to the first-order corrections in $1/m_Q$:

$$\lambda_H = \frac{1}{8}\left(M^2_{P^*} - M^2_P\right), \tag{19}$$

$$\lambda_S = \frac{1}{8}\left(M^2_{P_1'} - M^2_{P_0^*}\right), \tag{20}$$

$$\lambda_T = \frac{3}{16}\left(M^2_{P_2^*} - M^2_{P_1}\right), \tag{21}$$

$$\lambda_X = \frac{3}{16}\left(M^2_{P_2} - M^2_{P_1^*}\right), \tag{22}$$

$$\lambda_Y = \frac{5}{24}\left(M^2_{P_3} - M^2_{P_2'^*}\right), \tag{23}$$

$$\lambda_Z = \frac{5}{24}\left(M^2_{P_3^*} - M^2_{P_2'}\right), \tag{24}$$

$$\lambda_R = \frac{7}{32}\left(M^2_{P_4^*} - M^2_{P_3'^*}\right). \tag{25}$$

In HQET, at 1 GeV scale the flavor symmetry spontaneously arises for b (bottom quark) and c (charm quark), and hence the elegance of flavor symmetry implies

$$\Delta_F^{(c)} = \Delta_F^{(b)}, \tag{26}$$

$$\lambda_F^{(c)} = \lambda_F^{(b)}. \tag{27}$$

The decays $F \to H + M$ (F = H, S, T, X, Y, Z, R, with M representing a light pseudoscalar meson) can be described by effective Lagrangians explained in terms of the fields introduced in Eqs. (1)–(7) that are valid at leading order in the heavy quark mass and light meson momentum expansion:

$$L_{HH} = g_{HH}\mathrm{Tr}\left\{\overline{H}_a H_b \gamma_\mu \gamma_5 A^\mu_{ba}\right\}, \tag{28}$$

$$L_{TH} = \frac{g_{TH}}{\Lambda}\mathrm{Tr}\left\{\overline{H}_a T^\mu_b (iD_\mu \not{A} + i\not{D} A_\mu)_{ba}\gamma_5\right\} + h.c., \tag{29}$$

$$L_{XH} = \frac{g_{XH}}{\Lambda}\mathrm{Tr}\left\{\overline{H}_a X^\mu_b (iD_\mu \not{A} + i\not{D} A_\mu)_{ba}\gamma_5\right\} + h.c., \tag{30}$$

$$L_{YH} = \frac{1}{\Lambda^2}\mathrm{Tr}\left\{\overline{H}_a Y^{\mu\nu}_b \left[k_1^Y\{D_\mu, D_\nu\}A_\lambda + k_2^Y(D_\mu D_\lambda A_\nu + D_\nu D_\lambda A_\mu)\right]_{ba}\gamma^\lambda\gamma_5\right\} + h.c., \tag{31}$$

$$L_{ZH} = \frac{1}{\Lambda^2}\mathrm{Tr}\left\{\overline{H}_a Z^{\mu\nu}_b \left[k_1^Z\{D_\mu, D_\nu\}A_\lambda + k_2^Z(D_\mu D_\lambda A_\nu + D_\nu D_\lambda A_\mu)\right]_{ba}\gamma^\lambda\gamma_5\right\} + h.c., \tag{32}$$

$$\begin{aligned} L_{RH} = \frac{1}{\Lambda^3}\mathrm{Tr}\{\overline{H}_a R^{\mu\nu\rho}_b [&k_1^R\{D_\mu, D_\nu D_\rho\}A_\lambda + k_2^R(\{D_\mu, D_\rho\}D_\lambda A_\nu \\ &+ \{D_\nu, D_\rho\}D_\lambda A_\mu + \{D_\mu, D_\nu\}D_\lambda A_\rho)]_{ba}\gamma^\lambda\gamma_5\} + h.c. \end{aligned} \tag{33}$$

In these equations, $D_\mu = \partial_\mu + V_\mu$, $\{D_\mu, D_\nu\} = D_\mu D_\nu + D_\nu D_\mu$, and $\{D_\mu, D_\nu D_\rho\} = D_\mu D_\nu D_\rho + D_\mu D_\rho D_\nu + D_\nu D_\mu D_\rho + D_\nu D_\rho D_\mu + D_\rho D_\mu D_\nu + D_\rho D_\nu D_\mu$. Λ is the chiral symmetry-breaking scale, taken as 1 GeV. g_{HH}, g_{SH}, g_{TH}, $g_{YH} = k_1^Y + k_2^Y$, and $g_{ZH} = k_1^Z + k_2^Z$ are the strong coupling constants involved. Using the Lagrangians L_{HH}, L_{SH}, L_{TH}, L_{YH}, L_{ZH}, and L_{RH}, the two-body strong decays of $Q\overline{q}$ heavy-light bottom mesons are given as $(2^+, 3^+) \to (0^-, 1^-) + M$,

$$\Gamma(2^+ \to 1^-) = C_M \frac{8g^2_{ZH}}{75\pi f_\pi^2 \Lambda^4}\frac{M_f}{M_i}\left[p_M^5\left(m_M^2 + p_M^2\right)\right], \tag{34}$$

$$\Gamma(2^+ \to 0^-) = C_M \frac{4g^2_{ZH}}{25\pi f_\pi^2 \Lambda^4}\frac{M_f}{M_i}\left[p_M^5\left(m_M^2 + p_M^2\right)\right], \tag{35}$$

$$\Gamma(3^+ \to 1^-) = C_M \frac{4g_{ZH}^2}{15\pi f_\pi^2 \Lambda^4} \frac{M_f}{M_i} \left[p_M^5 \left(m_M^2 + p_M^2 \right) \right], \tag{36}$$

and $(3^+, 4^+) \to (0^-, 1^-) + M$,

$$\Gamma(3^+ \to 1^-) = C_M \frac{36g_{RH}^2}{35\pi f_\pi^2 \Lambda^6} \frac{M_f}{M_i} \left[p_M^9 \right], \tag{37}$$

$$\Gamma(4^+ \to 1^-) = C_M \frac{4g_{RH}^2}{7\pi f_\pi^2 \Lambda^6} \frac{M_f}{M_i} \left[p_M^9 \right], \tag{38}$$

$$\Gamma(4^+ \to 0^-) = C_M \frac{16g_{RH}^2}{35\pi f_\pi^2 \Lambda^6} \frac{M_f}{M_i} \left[p_M^9 \right], \tag{39}$$

where M_i, M_f represent the initial and final momentum, and Λ is the chiral symmetry-breaking scale of 1 GeV. p_M, m_M denote the final momentum and mass of the light pseudoscalar meson. The coupling constant plays the key role in phenomenological study of heavy light mesons. These dimensionless coupling constants describe the strength of the transition between the H–H field (negative–negative parity), S–H field (positive–negative parity), and T–H field (positive–negative parity). The coefficients C_M for different pseudoscalar particles are: $C_{\pi^\pm}$, $C_{K^\pm}$, C_{K^0}, $C_{\overline{K}^0} = 1$, $C_{\pi^0} = \frac{1}{2}$, and $C_\eta = \frac{2}{3}(c\bar{u}, c\bar{d})$ or $\frac{1}{6}(c\bar{s})$. In this paper we are not including higher-order corrections of $\frac{1}{m_Q}$ to bring new couplings. We also expect that higher corrections give small contributions in comparison to leading-order contributions.

3. Numerical analysis

Recently observed states like $D_0(2560)$, $D_1^*(2680)$, $D_2(2740)$, $D_3^*(2760)$, $D_J(3000)$, $D_J^*(3000)$ and strange states $D_{s1}(2860)$, $D_{s3}(2860)$, $D_s(3040)$ have a stimulated charm sector, but in the case of the bottom sector there are fewer experimental states compared to the charm sector. The newly observed excited strange bottom meson states $B_{sJ}(6064)$ and $B_{sJ}(6114)$ have developed the interest of theoreticians to study excited states of the bottom sector. With recent data from different experimental facilities, we are motivated to predict the masses and upper bounds of the coupling constants for $1F$ bottom meson states with strange partners in the framework of HQET.

In this paper, the analysis for $1F$ bottom meson states is based on two aspects: the masses of non-strange and strange $1F$ bottom meson states, and the decay behavior and channels of these states.

3.1 *Masses*

To describe the spectroscopy of bottom and bottom-strange mesons, mass is one important parameter. Input values used for calculating masses of $1F$ bottom states are listed in Table 1 with mentioned references.

To compute the masses of the $1F$ bottom states, we first calculated the values of the averaged masses $\overline{M_H}$, $\overline{M_Z}$, $\overline{M_R}$ introduced in Eqs. (10–17) for charm meson states from Table 1, then the HQS parameters Δ_Z, Δ_R, λ_Z, and λ_R described in Eqs. (10, 24, 25) are calculated for same charm meson states. The parameters Δ_F, λ_F are flavor independent in HQET, which implies $\Delta_F^{(c)} = \Delta_F^{(b)}$, $\lambda_F^{(c)} = \lambda_F^{(b)}$. With the calculated symmetry parameters Δ_F, λ_F for the charm mesons, and then applying heavy quark symmetry, we predicted the masses for the $1F$ bottom mesons listed in Table 2. For the details, we elaborate the calculation part of the mass

Table 1. Input values used in this work. All values are in units of MeV.

State	J^P	$c\overline{q}$	$c\overline{s}$	$b\overline{q}$	$b\overline{s}$
1^1S_0	0^-	1869.5 [6]	1969.0 [6]	5279.5 [6]	5366.91 [6]
1^3S_1	1^-	2010.26 [6]	2106.6 [6]	5324.71 [6]	5415.8 [6]
1^3F_2	2^+	3132 [41]	3208 [41]	–	–
$1F_3$	3^+	3143 [41]	3218 [41]	–	–
$1F_3^{'}$	3^+	3108 [41]	3186 [41]	–	–
1^3F_4	2^+	3113 [41]	3190 [41]	–	–

Table 2. Obtained masses for $1F$ bottom mesons

J^P	Masses of $1F$ bottom mesons (MeV)					
	Non-strange			Strange		
	Calculated	[10]	[23]	Calculated	[10]	[23]
$2^+(1^3F_2)$	6473.6	6412	6387	6518.28	6501	6358
$3^+(1F_3)$	6478.93	6420	6396	6523.21	6515	6369
$3^+(1F_3^{'})$	6447.76	6391	6358	6506.05	6468	6318
$4^+(1^3F_4)$	6450.14	6380	6364	6508.01	6475	6328

Table 3. Values of symmetry parameters.

Parameters	Our calculations	Ref. [10]	Ref. [23]
Δ_Z (MeV)	1163.35	1103.31	1078.89
Δ_R (MeV)	1135.74	1071.45	1048.02
λ_Z(GeV^2)	0.014	0.021	0.023
λ_R(GeV^2)	0.007	-0.03	0.017

of $B(1^3F_2)$. From Table 1, using the charm states we calculated $\overline{M_H^c} = 1975.07$ MeV, $\overline{M_Z^c} = 3138.42$ MeV. Then, using these two values, we have $\Delta_Z^{(c)} = \overline{M_Z^c} - \overline{M_H^c} = 1163.35$ MeV. Using Eq. (24) we get $\lambda_Z^{(c)} = 14380.2$ MeV^2. The symmetry of these parameters given by Eqs. (26) and (27) implies that $\Delta_Z^{(b)} = 1163.35$ MeV and $\lambda_Z^{(b)} = 14380.2$ MeV^2. Similarly, from Table 1 we calculated $\overline{M_H^b} = 5313.36$ MeV for bottom mesons. Using the values of $\Delta_Z^{(b)} = 1163.35$ MeV, $\lambda_Z^{(b)} = 14380.2$ MeV^2, and $\overline{M_H^b} = 5313.36$ MeV, we obtained the masses of the $1F$ bottom mesons listed in Table 2. For comparison, predictions from different models are also mentioned in Table 2. The masses obtained using the heavy quark symmetry in our work are in agreement with the masses obtained by the relativistic quark model in Ref .[10] with deviation of ±1.2% for non-strange states while strange states deviated by ±0.6%. On comparing with Ref. [23], our results deviated by ±3%. So, our results are in overall good agreement with other theoretical models. We have also explored symmetry parameters (Δ_F, λ_F) by taking different mass sets from Table 2. The computed values of the parameters are listed in Table 3. The parameters Δ_Z, Δ_R are consistent for different predicted theoretical masses from Table 2. The parameters λ_Z, λ_R are also close to each other for the same sets of masses. As λ_Z, λ_R are responsible for hyperfine splittings of the Z and R fields respectively, we find the masses of the $1F$ states with the above parameters are in reasonable agreement with other theoretical estimates.

3.2 *Decay widths*

By using the obtained masses, we computed the decay width for $1F$ bottom mesons via pseudoscalar particles (π, η, K) in the form of coupling constants. The formulation for the decay widths is discussed in Sect. 2. These decay width formulas are for strong decays via pseudoscalar particles only. The input values used for calculating the decay widths are $M_{\pi^0} = 134.97$ MeV, $M_{\pi^+} = 139.57$ MeV, $M_{K^+} = 493.67$ MeV, $M_{\eta^0} = 547.85$ MeV, $M_{K^0} = 497.61$ MeV, $M_{B^{*\pm}} = 5324.70 \pm 0.12$ MeV, $M_{B^{\mp}} = 5279.34 \pm 0.12$ MeV, $M_{B_S^0} = 5366.88 \pm 0.14$ MeV, and$M_{B_S^{*\pm}} = 5415.40$ MeV, and the calculated masses for F-wave and bottom mesons are listed in Table 2.

The computed strong decay widths in the form of the coupling constants g_{ZH}, g_{RH} for $1F$ bottom mesons are collected in Tables 4 and 5. The weak and radiative decays are not included for the computed decay widths of bottom meson states. We also exclude decays via emissions of vector mesons (ω, ρ, K^*, ϕ). So, on comparing these computed strong decay widths with theoretical available total decay widths [41] we get upper bounds for the associated couplings (g_{ZH}, g_{RH}). The coupling constant plays an important role in hadron spectroscopy. Here, the dimensionless coupling constants g_{ZH}, g_{RH} give the strengths of transitions between Z–H fields and R–H fields, respectively. The values of the coupling constants are more for ground state transitions (H–H fields) than excited state (S–H, T–H, X–H, Z–H, R–H fields) transitions, as shown by the values of $g_{HH} = 0.64 \pm 0.075$ [40] while $g_{SH} = 0.56 \pm 0.04$, $g_{TH} = 0.43 \pm 0.01$ [40], $g_{XH} = 0.24$ [33]. Also, the values of the coupling constants are low at higher orders ($n = 2, 3$) in comparison with lower-order ($n = 1$) interactions [40,42,43] like $\tilde{g}_{HH} = 0.28 \pm 0.015$, $\tilde{g}_{sH} = 0.18 \pm 0.01$, and so on. This progression also supports the values of the coupling constants computed here. A particular state like B(6473) gives $22538.78 g^2_{ZH}$ total decay width; when compared with total decay widths calculated by other theoretical papers [41], we have provided an upper bound on the g_{ZH} value. Now, if we add additional modes, then the value of g_{ZH} may be less than 0.09 ($g_{ZH} < 0.09$). So, these upper bounds may give important information to other associated bottom states. Without enough experimental information, it is not possible to compute the values of coupling constants from heavy quark symmetry entirely, but upper bounds for these couplings are mentioned in Tables 4 and 5. Here, we need to emphasize that the computed total decay widths for the above states do not include contributions from decays via emission of vector mesons (ω, ρ, K^*, ϕ) since the contributions of vector mesons to total decay widths are smaller than pseudoscalar mesons. They give contributions of ± 50 MeV to the total decay widths for the states analyzed above [23]. Further, we now discuss Regge trajectories which justify our calculated masses for the $1F$ bottom meson states.

3.3 *Regge trajectory*

The Regge trajectory is an effective phenomenological approach to describing hadron spectroscopy. A plot between total angular momentum (J) and radial quantum number (n_r) of hadrons against the square of their masses (M^2) provides information about the quantum number of a particular state and also helps to identify recently observed states. We use the following definitions:

(a) The (J, M^2) Regge trajectories:

$$J = \alpha M^2 + \alpha_0. \tag{40}$$

Table 4. Decay width of obtained masses for $1F$ non-strange bottom mesons.

States	J^P	Decay modes	Decay widths	Total decay width [MeV] [41]	Upper bound of coupling constant
$B(6473.6)$	2^+	$B^{*+}\pi^-$	$3347.69g^2_{ZH}$		
		$B^{*0}\pi^0$	$1672.14g^2_{ZH}$		
		$B^{*0}\eta^0$	$1367.92g^2_{ZH}$		
		$B^*_sK^0$	$1328.31g^2_{ZH}$		
		$B^+\pi^-$	$6262.1g^2_{ZH}$		
		$B^0\eta^0$	$2657.76g^2_{ZH}$		
		$B^0_sK^0$	$2774.61g^2_{ZH}$		
		$B^0\pi^0$	$3128.25g^2_{ZH}$		
		Total	$22538.78g^2_{ZH}$		
			g_{ZH}	202.4	0.09
$B(6478.93)$	3^+	$B^{*0}\pi^0$	$4609.40g^2_{ZH}$		
		$B^{*+}\pi^-$	$9201.01g^2_{ZH}$		
		$B^{*0}\eta^0$	$3823.83g^2_{ZH}$		
		$B^{*0}_sK^0$	$3700.1g^2_{ZH}$		
		Total	$21334.34g^2_{ZH}$		
			g_{ZH}	105.2	0.07
$B(6447.76)$	3^+	$B^{*0}\pi^0$	$29675g^2_{RH}$		
		$B^{*+}\pi^-$	$14898.6g^2_{RH}$		
		$B^{*0}\eta^0$	$7117.82g^2_{RH}$		
		$B^{*0}_sK^0$	$5933.87g^2_{RH}$		
		Total	$57625.29g^2_{RH}$		
			g_{RH}	221.8	0.06
$B(6450.14)$	4^+	$B^{*+}\pi^-$	$16168g^2_{RH}$		
		$B^{*0}\pi^0$	$8117.39g^2_{RH}$		
		$B^{*0}\eta^0$	$3856.74g^2_{RH}$		
		$B^*_sK^0$	$3208.9g^2_{RH}$		
		$B^+\pi^-$	$21811.5g^2_{RH}$		
		$B^0\eta^0$	$5638.37g^2_{RH}$		
		$B^0_sK^0$	$5731.86g^2_{RH}$		
		$B^0\pi^0$	$10925.9g^2_{ZH}$		
		Total	$22538.78g^2_{ZH}$		
			g_{RH}	110.0	0.07

(b) The (n_r, M^2) Regge trajectories:

$$n_r = \beta M^2 + \beta_0. \tag{41}$$

Here, α and β are slopes, and α_0 and β_0 are intercepts. We plot the Regge trajectories in the plane (J, M^2) with natural parity $P = (-1)^J$ and unnatural parity $P = (-1)^{J-1}$ for $1F$ bottom mesons using the predicted spectroscopic data. The plots of Regge trajectories in the (J, M^2) plane are also known as Chew–Frautschi plots [44–46]. The plots are shown in Figs. 1–4, where the masses for S-wave and P-wave(1^+, 2^+) are taken from the Particle Data Group; the remaining masses are taken from Ref. [14], and for $1F$ we are taking our calculated

Table 5. Decay width of obtained masses for 1F strange bottom mesons.

States	J^P	Decay modes	Decay widths	Total decay width [MeV] [41]	Upper bound of coupling constant
$B_s(6518.28)$	2^+	$B^{*0}K^0$	$1850.44g^2_{ZH}$		
		$B^{*-}K^+$	$1864.99g^2_{ZH}$		
		$B_s^{*0}\eta^0$	$152.47g^2_{ZH}$		
		$B_s^{*}\pi^0$	$861.63g^2_{ZH}$		
		B^0K^0	$3601.08g^2_{ZH}$		
		B^-K^+	$3632.92g^2_{ZH}$		
		$B_s^0\eta^0$	$317.73g^2_{ZH}$		
		$B_s^0\pi^0$	$1687.81g^2_{ZH}$		
		Total	$13969.07g^2_{ZH}$		
			g_{ZH}	256.3	0.13
$B_s(6523.21)$	3^+	$B^{*-}K^+$	$4762.7g^2_{ZH}$		
		$B^{*0}K^0$	$4727.53g^2_{ZH}$		
		$B_s^{*0}\eta^0$	$394.77g^2_{ZH}$		
		$B_s^{*0}\pi^0$	$2216.24g^2_{ZH}$		
		Total	$12101.24g^2_{ZH}$		
			g_{ZH}	138.4	0.10
$B_s(6506.05)$	3^+	$B^{*-}K^+$	$12627.5g^2_{RH}$		
		$B^{*0}K^0$	$12434.2g^2_{RH}$		
		$B_s^{*0}\eta^0$	$714.78g^2_{RH}$		
		$B_s^{*0}\pi^0$	$7469.58g^2_{RH}$		
		Total	$33,246.06g^2_{RH}$		
			g_{RH}	274	0.09
$B_s(6508.01)$	4^+	$B^{*0}K^0$	$7023.53g^2_{RH}$		
		$B^{*-}K^+$	$7131.87g^2_{RH}$		
		$B_s^{*0}\eta^0$	$405.17g^2_{RH}$		
		$B_s^{*}\pi^0$	$4211.83g^2_{RH}$		
		B^0K^0	$8073.71g^2_{RH}$		
		B^-K^+	$8207.52g^2_{RH}$		
		$B_s^0\eta^0$	$518.27\ g^2_{RH}$		
		$B_s^0\pi^0$	$4787.05g^2_{RH}$		
		Total	$40358.95g^2_{RH}$		
			g_{RH}	138.6	0.05

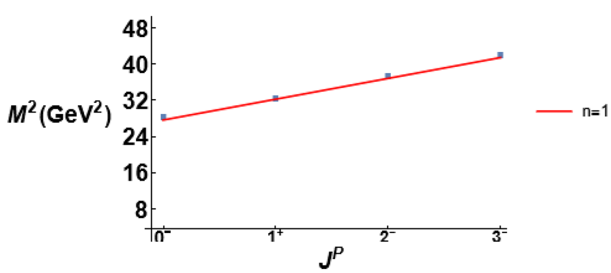

Fig. 1. Regge trajectories for non-strange bottom mesons with unnatural parity in the plane ($M^2 \to J^P$).

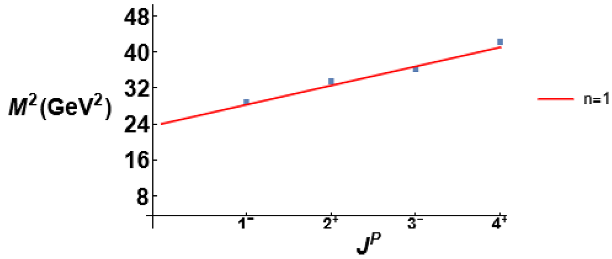

Fig. 2. Regge trajectories for non-strange bottom mesons with natural parity in the plane ($M^2 \rightarrow J^P$).

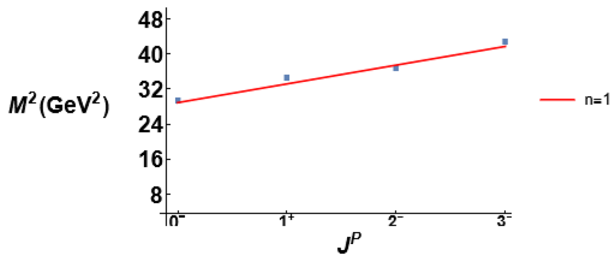

Fig. 3. Regge trajectories for strange bottom mesons with unnatural parity in the plane ($M^2 \rightarrow J^P$).

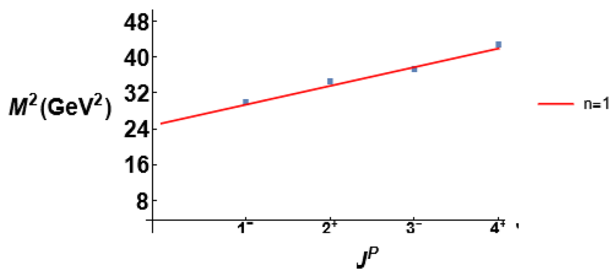

Fig. 4. Regge trajectories for strange bottom mesons with natural parity in the plane ($M^2 \rightarrow J^P$).

Table 6. Regge slopes and intercepts

Figure	Slope (α) [MeV^{-2}]	Intercepts (α_0)
1	0.194717	−5.30365
2	0.217415	−5.07794
3	0.22186	−6.52136
4	0.235764	−5.90507

masses. As Regge trajectories are known to be linear for mesons, this supports our obtained results and also helps to define the spin parity state to higher resonance since the Regge lines are almost linear, parallel, and equidistant in Figs. 1–4. The Regge slopes (α) and intercepts α_0 are listed in Table 6. Our results nicely fit on Regge lines, which also justifies the authenticity of the HQET formulation.

4. Conclusion

Heavy quark symmetry is an important tool in describing the spectroscopy of hadrons. Using available experimental as well as theoretical data on charm mesons and applying HQS, we computed masses for $1F$ bottom meson spectra. With the predicted masses of $1F$ bottom mesons, we analyzed decay widths for 1*F* with emission of pseudoscalar mesons and presented the decay widths in the form of coupling constants. These coupling constants are estimated on comparing our decay widths with available theoretical total decay widths. The total decay widths may give an upper bound on these coupling constants, hence providing a useful clue to other associated states of bottom mesons. Using our calculated bottom masses for 1*F*, we constructed Regge trajectories in the (J, M^2) plane. Our predicted data fit them nicely. Our calculated masses and upper bound findings may help experimentalists looking into higher excited states.

Acknowledgment

The authors gratefully acknowledge the financial support of the Department of Science and Technology (SERB/F/9119/2020), New Delhi.

Funding

Open Access funding: SCOAP^3.

References

[1] R. Aaij et al.[LHCb Collaboration], Phys. Rev. Lett. **126**, 122002 (2021).
[2] P. del Amo Sanchez et al.[BaBar Collaboration], Phys. Rev. D **82**, 111101(R) (2010).
[3] R. Aaij et al.[LHCb Collaboration], J. High Energy Phys. **09**, 145 (2013).
[4] R. Aaij et al.[LHCb Collaboration], Phys. Rev. D **101**, 032005 (2020).
[5] R. Aaij et al.[LHCb Collaboration], Phys. Rev. D **94**, 072001 (2016).
[6] P. A. Zyla et al.[Particle Data Group], Prog. Theor. Exp. Phys. **2020**, 083C01 (2020).
[7] T. A. Aaltonen et al.[CDF Collaboration], Phys. Rev. D **90**, 012013 (2014).
[8] R. Aaij et al.[LHCb Collaboration], J. High Energy Phys. **04**, 024 (2015).
[9] R. Aaij et al. Eur.Phys.J.C **81**,601 (2021)
[10] D. Ebert, R. N. Faustov, and V. O. Galkin, Eur. Phys. J. C **66**, 197 (2010).
[11] J. B. Liu and C. D. Lü, Eur. Phys. J. C **77**, 312 (2017).
[12] C. B. Lang, D. Mohler, S. Prelovsek, and R. M. Woloshyn, Phys. Lett. B **750**, 17 (2015).
[13] E. B. Gregory et al., Phys. Rev. D **83**, 014506 (2011).
[14] Q. Li, R.-H. Ni, and X.-H. Zhong, Phys. Rev. D **103**, 116010 (2021).
[15] D. Jia and W. C. Dong, Eur. Phys. J. Plus **134**, 123 (2019).
[16] H. Y. Cheng and F. S. Yu, Eur. Phys. J. C **77**, 668 (2017).
[17] M. H. Alhakami, Phys. Rev. D **103**, 034009 (2021).
[18] Y. Lu, M. N. Anwar, and B. S. Zou, Phys. Rev. D **95**, 034018 (2017).
[19] B. H. Yazarloo and H. Mehraban, Europhys. Lett. **116**, 31004 (2016).
[20] M. Shah, B. Patel, and P. C. Vinodkumar, Phys. Rev. D **93**, 094028 (2016).
[21] M. Di Pierro and E. Eichten, Phys. Rev. D **64**, 114004 (2001).
[22] Y. Sun, Q. T. Song, D. Y. Chen, X. Liu, and S. L. Zhu, Phys. Rev. D **89**, 054026 (2014).
[23] S. Godfrey, K. Moats, and E. S. Swanson, Phys. Rev. D **94**, 054025 (2016).
[24] Q. F. Lü, T. T. Pan, Y. Y. Wang, E. Wang, and D. M. Li, Phys. Rev. D **94**, 074012 (2016).
[25] I. Asghar, B. Masud, E. S. Swanson, F. Akram, and M. A. Sultan, Eur. Phys. J. A **54**, 127 (2018).
[26] S. Godfrey and K. Moats, Eur. Phys. J. A **55**, 84 (2019).
[27] Z. H. Wang, Y. Zhang, T. H. Wang, Y. Jiang, Q. Li, and G. L. Wang, Chin. Phys. C **42**, 123101 (2018).
[28] G. L. Yu and Z. G. Wang, Chin. Phys. C **44**, 033103 (2020).
[29] H. A. Alhendi, T. M. Aliev, and M. Savci, J. High Energy Phys. **04**, 050 (2016).
[30] J. Ferretti and E. Santopinto, Phys. Rev. D **97**, 114020 (2018).
[31] Z. G. Wang, Eur. Phys. J. C **74**, 3123 (2014).
[32] H. Xu, X. Liu, and T. Matsuki, Phys. Rev. D **89**, 097502 (2014).
[33] Z. G. Wang, Eur. Phys. J. Plus **129**, 186 (2014).
[34] J. M. Zhang and G. L. Wang, Phys. Lett. B **684**, 221 (2010).
[35] Z. G. Luo, X. L. Chen, and X. Liu, Phys. Rev. D **79**, 074020 (2009).

[36] P. Gupta and A. Upadhyay, Proc. Sci. **2018**, 025 (2018).
[37] P. Gupta and A. Upadhyay, Phys. Rev. D **99**, 094043 (2019).
[38] S. L. Zhu and Y. B. Dai, Mod. Phys. Lett. A **14**, 2367 (1999).
[39] B. Chen et al., Phy. Rev.D **105**,074014 (2022).
[40] P. Colangelo, F. De Fazio, F. Giannuzzi, and S. Nicotri, Phys. Rev. D **86**, 054024 (2012).
[41] S. Godfrey and K. Moats, Phys. Rev. D **93**, 034035 (2016).
[42] R. Casalbuoni, A. Deandrea, N. Di Bartolomeo, F. Feruglio, R. Gatto, and G. Nardulli, Phys. Rep. **281**, 145 (1997).
[43] R. Garg, Prog. Theor. Exp. Phys. **2022**, 043B06 (2022).
[44] G. F. Chew and S. C. Frautschi, Phys. Rev. Lett. **7**, 394 (1961).
[45] Y. Nambu, Phys. Rev. D **10**, 4262 (1974).
[46] Y. Nambu, Phys. Lett. B **80B**, 372 (1979).